Multipurpose Near- and Far-Field Switched Multiband Coil Antenna for 915-MHz/2.45/5.8-GHz RFIDs

Ashwani Sharma, Ignacio J. Garcia Zuazola, *Senior Member, IEEE*, and Asier Perallos

***Abstract*—A multipurpose near- and far-field switched multiband reader antenna for radio frequency identification (RFID) applications is presented. The proposed antenna is simple, planar, and has three modes of operating frequencies: 915 MHz, 2.45 GHz, and 5.8 GHz. The prototype is realized using nonuniformly distributed turns coil for robust reactive and radiated field performance, leading to a multipurpose near- and far-field antenna in a single unit. Results show performance of the proposed multipurpose antenna in both near-field and far-field region and demonstrate its suitability for various RFID applications.**

***Index Terms*—Far field (FF), H-field, loop antenna, near field (NF), radio frequency identification (RFID), switched multiband response.**

I. Introduction

RADIO frequency identification (RFID) technology is considered as an attractive solution for tracking and tracing applications. The typical RFID provides contactless transfer of the information between an interrogator (Reader) and a transponder (Tag) tuned at the same frequency of operation. Depending on the application, various frequency bands have been adopted for RFID operation—e.g., HF: 13.56 MHz, UHF: 866/915 MHz, Microwave: 2.45 GHz, 5.8 GHz. In addition to the operating frequency, the RFID systems are categorized by the region of operation, e.g., near field (NF) and far field (FF). The NF RFIDs are used for short-range interrogation while employing inductive coupling between the tag and the reader antennas [1]. Therefore, coil antennas are used as low-cost solution. Conversely, the FF RFIDs are applicable for long-range interrogation employing back-scattering technique where a descent FF radiation is expected from the reader antenna. In general, specific RFID antennas are designed for specific applications operating at a particular frequency and optimized for either NF or FF performance. However, low-cost multipurpose antennas having both NF and FF operations along with multiband response are highly desirable.

In the literature, several designs of RFID antennas with various combinations of NF, FF, and multiband responses are present. For instance, single-band antennas with solely NF operation were proposed in [2] and [3] at UHF 915 and 866 MHz, and in [4] at 2.45 GHz. Meanwhile, antennas functioning at UHF having both NF and FF operations were presented in [5]–[8]. In contrast, the antennas with multiband response and solely FF operation were also designed, e.g., a dual-band antenna for 2.4/5.8 GHz [9], triband antennas for 433/923 MHz/2.45 GHz [10] and 3.6/5.8/8.2 GHz [11] were presented. Moreover, a dual-band RFID antenna proposed in [12] was designed to operate in NF at HF 13.56 MHz and FF at UHF 920 MHz. In [13], Sharma *et al.* have presented a switched dual-band coil antenna working in NF at HF and FF at UHF, where the radii of inner turns of the coil were optimized using nonuniformly distributed turns [14] terminology for a maximum H-field in the interrogation zone. Therefore, the reader antenna presented here is intended to provide maximum H-field in the interrogation zone and not necessarily over a large interrogation zone; for robust H-field with three orthogonal H-field components in larger interrogation zones, the authors have suggested using planar multicoil antennas in [15]. This review suggests that the reconfigurable antennas having multiband response with switchable operating frequencies are of much interest to reduce interference and system cost and to improve system performance [16].

In this letter, a switched multiband antenna is proposed in Section II operating both in NF and FF, thus having multiple utilities. The proposed antenna is designed to switch between three operating frequencies 915 MHz, 2.45 GHz, and 5.8 GHz using RF switches, which leads to a multipurpose NF and FF antenna in a single unit. The proposed antenna is simple and fabricated on a single-sided printed circuit board (PCB). The results in Section III include the H-field (in NF) and radiation pattern (in FF) performance in each switching state of the antenna to prove the usefulness of the proposed design for various NF and FF RFID applications. The fabricated antenna and measurements are presented in Section IV. The letter is concluded in Section V.

II. Multipurpose Switched Multiband Antenna

The proposed switched multiband NF–FF antenna shown in Fig. 1 was designed by incorporating a coil with nonuniformly distributed turns etched on a single-sided PCB of copper (50 μm), FR4 substrate ($E_r = 4.8$ and $\tan\delta = 0.02$), and thickness $h = 0.8$ mm. The coil antenna of size $98 \times 98 \times 0.8$ mm^3 lies

Manuscript received June 2, 2017; revised July 14, 2017; accepted July 19, 2017. Date of publication July 28, 2017; date of current version August 28, 2017. *(Corresponding author: Ashwani Sharma.)*

A. Sharma is with the Department of Electronics and Communication Engineering, Jaypee University of Information Technology, Waknaghat 173234, India, and also with Deusto Institute of Technology—DeustoTech, University of Deusto, Bilbao 48007, Spain (e-mail: ashwani.sharma@deusto.es).

I. J. Garcia Zuazola is with the School of Electronic, Electrical and Systems Engineering, Loughborough University, Loughborough LE11 3TU, U.K., and also with Deusto Institute of Technology—DeustoTech, University of Deusto, Bilbao 48007, Spain (e-mail: i.j.garcia-zuazola@lboro.ac.uk).

A. Perallos is with Deusto Institute of Technology—DeustoTech, University of Deusto, Bilbao 48007, Spain (e-mail: perallos@deusto.es).

Color versions of one or more of the figures in this letter are available online at http://ieeexplore.ieee.org.

Digital Object Identifier 10.1109/LAWP.2017.2733160

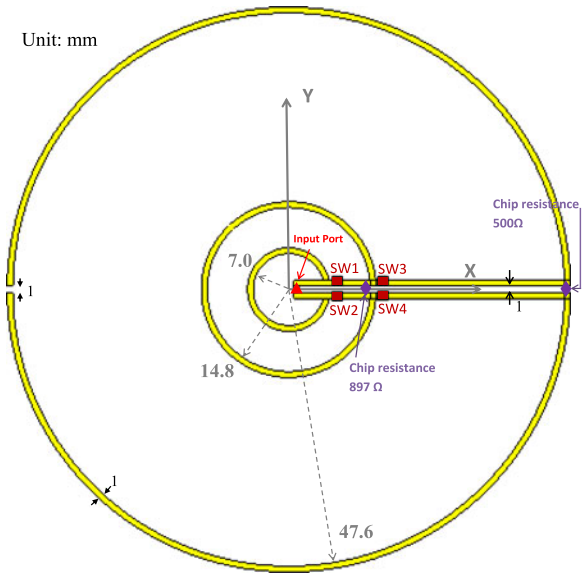

Fig. 1. Multipurpose switched multiband antenna.

TABLE I
SWITCHING BETWEEN MULTIPLE BANDS

Mode: Band	SW1	SW2	SW3	SW4
Mode-1: 915 MHz	ON	ON	ON	ON
Mode-2: 2.45 GHz	ON	ON	OFF	OFF
Mode-3: 5.80 GHz	OFF	OFF	OFF	OFF

in the *xy* plane with the center at the origin, as in Fig. 1. The antenna consists of three turns with radii [47.6, 14.8, 7.0] mm selected to achieve three operating frequencies, 915 MHz, 2.45 GHz, and 5.8 GHz, using RF switches SW1–4. Depending on the switching states (ON or OFF), the antenna has three modes of operation listed in Table I. In mode-3, when all the switches are OFF, the innermost turn isolates from other turns and the antenna resonates at 5.8 GHz. In mode-2, the antenna resonates at 2.45 GHz when the two inner turns are connected and contribute to NF and FF radiations. In mode-3, all the three turns are connected contributing to NF and FF radiation, and the operating frequency switches to 915 MHz. The chip resistances are selected to resonate the antenna at desired frequencies. The antenna is simulated and fabricated, and results are presented subsequently.

III. SIMULATION RESULTS

The antenna shown in Fig. 1 is simulated using CST MW studio. In this study, we have considered an ideal switch model where the OFF state is represented by an open circuit (no metal) and the ON state by a short circuit (galvanic connection with metal strip). The antenna performance is evaluated for all the modes of operation, and simulated S_{11} responses are shown in Fig. 2. The results show that the antenna resonates around 915 MHz in mode-1, 2.45 GHz in mode-2, and 5.8 GHz in mode-3. The simulated bandwidth corresponding to 25 dB return loss is 30 MHz (900–930 MHz) in mode-1, 70 MHz (2.42–2.49 GHz) in mode-2, and 340 MHz (5.59–5.93 GHz) in mode-3. For each mode, the antenna with input power 1 W is simulated to evaluate vertical H-field component (H_z) in NF zone and radiation pattern in FF zone of the antenna.

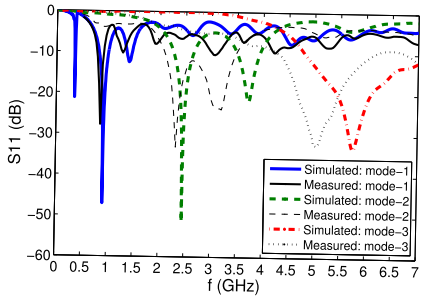

Fig. 2. S_{11} response of the switched multiband antenna.

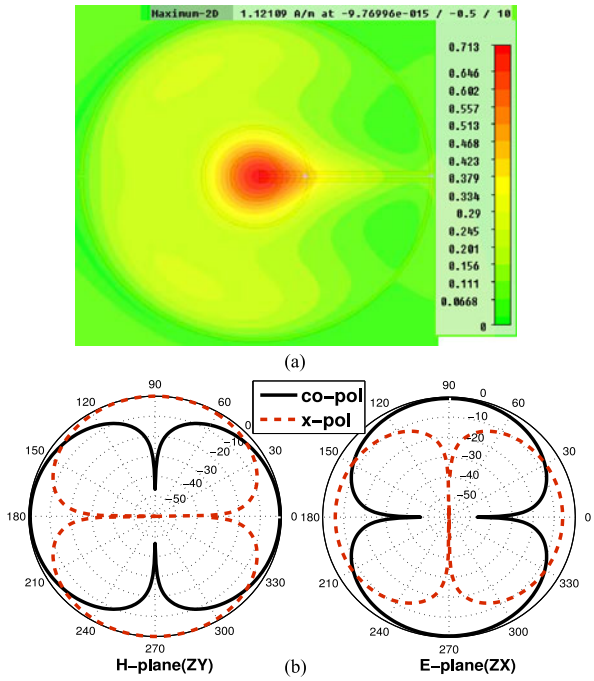

Fig. 3. Mode-1: Simulated (a) H_z in NF; (b) normalized FF radiation patterns.

A. Mode-1: UHF 915 MHz NF–FF Performance

In mode-1, the simulated H_z distribution of the antenna at 915 MHz is presented in Fig. 3(a) in $z = 10$ mm plane. The maximum H_z magnitude shown is 1.12 A/m. To assess FF performance, the simulated normalized radiation patterns are shown in Fig. 3(b). The results showed that the antenna in mode-1 has a maximum gain of ∼1 dBi in elevation plane.

B. Mode-2: 2.45 GHz NF–FF Performance

In mode-2, the antenna is simulated at 2.45 GHz, and Fig. 4(a) shows the simulated H_z distribution of the antenna in $z = 10$ mm plane. The maximum achieved H_z has magnitude 0.82 A/m. The FF simulation of the antenna in mode-2 generated normalized radiation patterns of Fig. 4(b) and showed a maximum gain of ∼4.1 dBi at 2.45 GHz.

C. Mode-3: 5.8 GHz NF–FF Performance

The proposed design is simulated in mode-3 at 5.8 GHz. The H_z distribution of the antenna in the $z = 10$ mm plane is shown in Fig. 5(a) where maximum achieved H_z has a magnitude 0.98 A/m. The FF simulated radiation patterns at 5.8 GHz are plotted in Fig. 5(b) and show a maximum gain of ∼4.3 dBi.

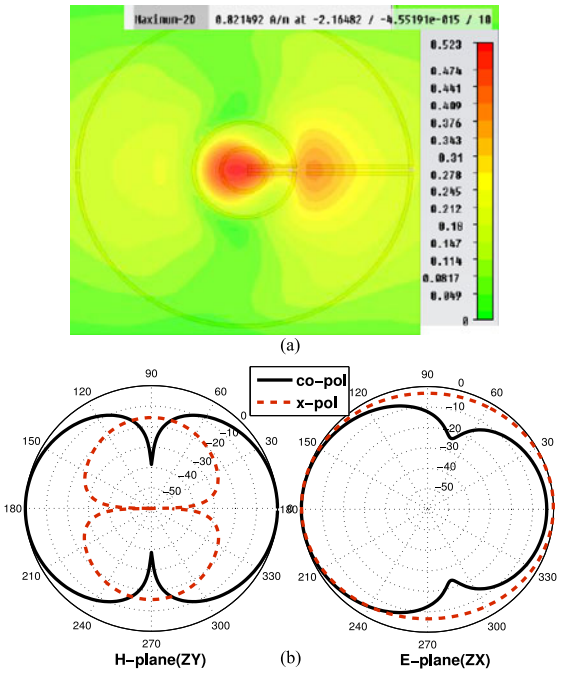

Fig. 4. Mode-2: Simulated (a) H_z in NF; (b) normalized FF radiation patterns.

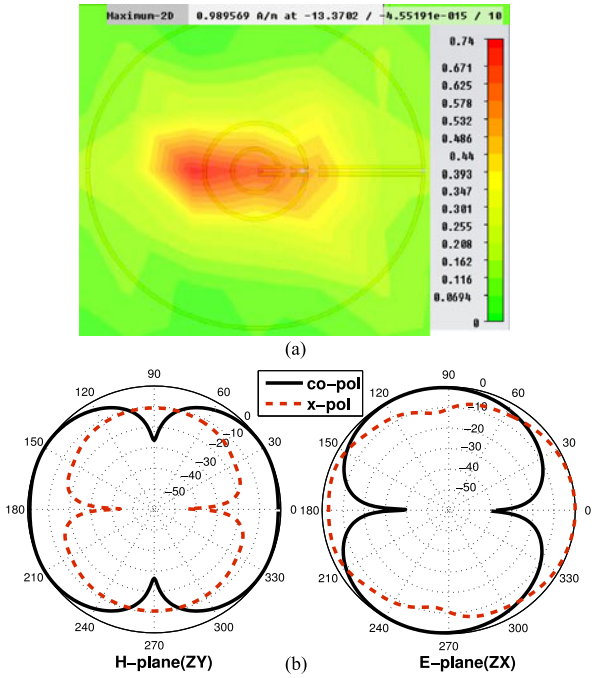

Fig. 5. Mode-3: Simulated (a) H_z in NF; (b) FF normalized radiation patterns.

IV. Antenna Fabrication and Measurements

The proposed antenna was fabricated and shown in Fig. 6. To measure the reflection coefficient (S_{11}) of the antenna, an Agilent PNA-X network analyzer (connectors and cables appropriately calibrated) was used. The measured S_{11} responses in three modes of operation are included in Fig. 2 and compared with simulated S_{11} responses. The deviation of measured S_{11} parameter at 5.8 GHz is attributed to the SMA connector that was not considered in the simulation and acted as a parasitic element affecting the response. The fabricated antenna is measured for NF and FF performance, subsequently.

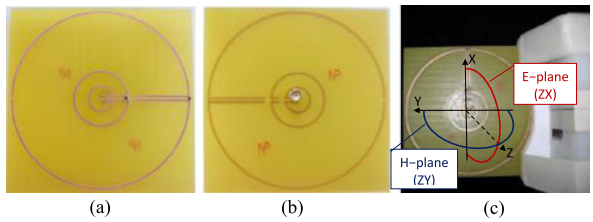

Fig. 6. Fabricated antenna. (a) Front view, (b) back view, and (c) radiation pattern measurements in anechoic chamber showing the antenna coordinates.

TABLE II
Measured NF and FF Results of the Proposed Antenna

Mode: Band	NF H_z (A/m)		FF Gain (dBi)	
	Simulated	Measured	Simulated	Measured
Mode-1: 915 MHz	1.12	1.24	1	1.1
Mode-2: 2.45 GHz	0.82	0.71	4.1	3.4
Mode-3: 5.80 GHz	0.98	Not available	4.3	3.8

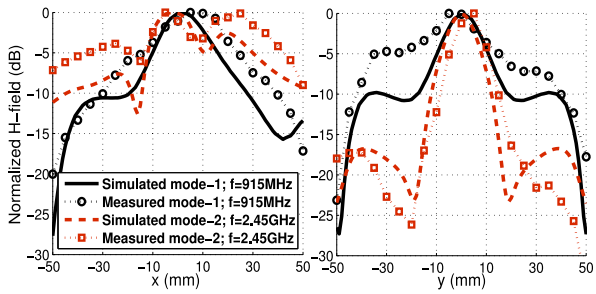

Fig. 7. Measured NF performance of the proposed antenna in $z = 10$ mm plane.

To assess NF performance, the H_z of the antenna in three modes were measured using NF probes (ETS-Lindgren's Model 7405 Set) placed at a distance $z = 10$ mm away from the antenna. The NF probes were connected to the network analyzer to measure received H_z. The FF performance was assessed by radiation pattern measurements in anechoic chamber with antenna coordinates, as shown in Fig. 6(c). The measured NF and FF performance of the proposed antenna is summarized in Table II and compared with the simulated results presented in Section III.

In the NF, the proposed antenna achieves a maximum of 1.24 and 0.71 A/m H-field in mode-1 and mode-2, respectively, at 10 mm distance from the antenna. Note that Table II does not include NF result in mode-3 due to unavailability of an NF probe functioning at 5.8 GHz in our measurement facility. However, the simulation results show that the proposed antenna is intended to perform well in mode-3.

The measured H_z distributions of the antenna in $z = 10$ mm plane (along x- and y-directions) are plotted in Fig. 7 for mode-1 and mode-2, which corroborate with the simulated NF distributions.

The measured FF results of Table II show that the proposed antenna has the maximum FF gain of 1.1 dBi in mode-1 at

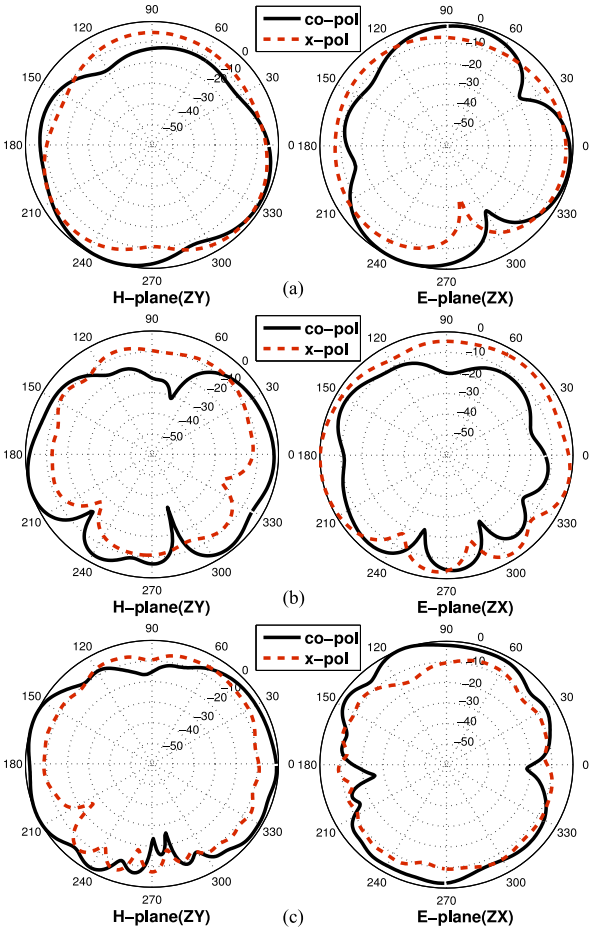

Fig. 8. Measured FF radiation patterns. (a) Mode-1. (b) Mode-2. (c) Mode-3.

915 MHz, 3.4 dBi in mode-2 at 2.45 GHz, and 3.8 dBi in mode-3 measured at 5.8 GHz. The measured FF radiation patterns of the antenna in three modes are plotted in Fig. 8 showing a wide E-total radiation pattern in the three modes of operation, which is in sync with the simulated radiation pattern results presented in Section III. Because RFID transponders/tags are generally linearly polarized, a circularly polarized reader would have a polarization loss factor of 0.5 (-3 dB) no matter what the angle the tag is rotated to. To ease this inevitable signal loss due to polarization mismatch, the two antennas (transponder and reader) had analogous linear polarization. This might limit the reader to applications where tags in the FF are oriented in a predefined direction, e.g., conveyer belt.

The results corroborated with the objectives of the design and showed that the proposed antenna with switching ability provides frequency agility between three frequency bands, hence a switched multiband operation is realized. Furthermore, the proposed antenna has a decent NF and FF performance proving its suitability for multipurpose NF and FF RFID applications.

V. Conclusion

A multipurpose switched multiband antenna used for NF and FF RFID applications is presented. The antenna incorporates frequency reconfigurability by switching between three frequency bands using four RF switches. Depending upon the states of the switches, one out of three modes 1–3 is selected with corresponding resonance frequency 915 MHz, 2.45 GHz, and 5.8 GHz, respectively. The loop shape is adopted in the design to generate effective reactive field (H-field) in the interrogation zone; this works for NF RFID applications. Meanwhile, the FF radiation is generated due to nonuniform currents along the loop making the antenna suitable for FF RFID applications. The switched multiband operation of the proposed antenna was evaluated using ideal switch model. The NF results showed the H-field of $\sim$1.12, 0.82, and 0.98 A/m at 10 mm distance from the antenna. Moreover, the FF results showed the gain of $\sim$1, 4.1, and 4.3 dBi achieved by the proposed design switched in modes 1–3, respectively. The antenna was fabricated and measured, and the results were corroborated. This demonstrates the suitability of the proposed antenna for multiple purposes (NF and FF) in addition to switching ability for frequency reconfigurability.

References

[1] Y. Lee, "Antenna circuit design for RFID applications," Microchip Technol. Inc., Chandler, AZ, USA, 2003. [Online]. Available: http://ww1.microchip.com/downloads/en/appnotes/00710c.pdf

[2] Z. N. Chen, C. K. Goh, and X. Qing, "Loop antenna for UHF near-field RFID reader," in *Proc. 4th Eur. Conf. Antenna Propag.*, Barcelona, Spain, Apr. 2010, pp. 1–4.

[3] A. Michel, M. R. Pino, and P. Nepa, "Reconfigurable modular antenna for NF UHF RFID smart point readers," *IEEE Trans. Antenna Propag.*, vol. 65, no. 2, pp. 498–506, Feb. 2017.

[4] X. Chen, W. G. Yeoh, Y. B. Choi, H. Li, and R. Singh, "A 2.45-GHz near-field RFID system with passive on-chip antenna tags," *IEEE Trans. Microw. Theory Techn.*, vol. 56, no. 6, pp. 1397–1404, Jun. 2008.

[5] B. Shrestha, A. Elsherbeni, and L. Ukkonen, "UHF RFID reader antenna for near-field and far-field operations," *IEEE Antennas Wireless Propag. Lett.*, vol. 10, pp. 1274–1277, 2011.

[6] X. Qing, Z. N. Chen, and C. K. Goh, "A UHF near-field/far-field RFID metamaterial-inspired loop antenna," in *Proc. IEEE Antennas Propag. Soc. Int. Symp.*, Chicago, IL, USA, Jul. 2012, pp. 1–2.

[7] A. C. de Souze, Y. Duroc, T. P. Vuong, A. Luce, and J. Perdereau, "A near-field and far-field antenna for UHF RFID applications," in *Proc. IEEE-APS Top. Conf. Antennas Propag. Wireless Commun.*, Turin, Italy, Sep. 2013, pp. 1240–1243.

[8] A. L. Borja, A. Belenguer, J. Cascon, and J. R. Kelly, "A reconfigurable passive UHF reader loop antenna for near-field and far-field RFID applications," *IEEE Antennas Wireless Propag. Lett.*, vol. 11, pp. 580–583, 2012.

[9] J. R. Panda and R. S. Kshetrimayum, "A printed 2.4 GHz/5.8 GHz dual-band monopole antenna for WLAN and RFID applications with a protruding stub in the ground plane," in *Proc. Nat. Conf. Commun.*, Bengaluru, India, Jan. 2011, pp. 1–5.

[10] F. Y. Zulkifli, S. F. Siddiq, and E. T. Rahardjo, "Multiband microstrip antenna for RFID application," in *Proc. IEEE Asia–Pac. Conf. Appl. Electromagn.*, Port Dickson, Malaysia, Nov. 2010, pp. 1–4.

[11] C. Varadhan, J. K. Pakkathillam, M. Kanagasabai, R. Sivasamy, R. Natarajan, and S. K. Palaniswamy, "Triband antenna structures for RFID systems deploying fractal geometry," *IEEE Antennas Wireless Propag. Lett.*, vol. 12, pp. 437–440, 2013.

[12] W. I. Son, K. S. Oh, W. S. Lee, H. S. Tae, and J. W. Yu, "Dual-frequency antenna for HF/UHF handheld RFID reader," in *Proc. IEEE MTT-S Int. Microw. Workshop Ser. Intell. Radio Future Pers. Terminals*, Daejeon, South Korea, Aug. 2011, pp. 1–2.

[13] A. Sharma, I. J. Garcia Zuazola, J. C. Batchelor, and A. Perallos, "Switched non-uniformly distributed-turns coil antenna for dual-band operation," in *Proc. 9th Eur. Conf. Antennas Propag.*, Lisbon, Portugal, Apr. 2015, pp. 1–4.

[14] A. Sharma, I. J. Garcia Zuazola, A. Gupta, A. Perallos, and J. C. Batchelor, "Non-uniformly distributed-turns coil antenna for enhanced H-field in HF RFID," *IEEE Trans. Antenna Propag.*, vol. 61, no. 10, pp. 4900–4907, Oct. 2013.

[15] A. Sharma, G. Singh, D. Bhatnagar, I. J. Garcia Zuazola, and A. Perallos, "Magnetic-field forming using planar multi-coil antenna to generate orthogonal H-field components," *IEEE Trans. Antenna Propag.*, vol. 65, no. 6, pp. 2906–2915, Jun. 2017.

[16] R. L. Haupt and M. Lanagan, "Reconfigurable antennas," *IEEE Antennas Propag. Mag.*, vol. 55, no. 1, pp. 49–61, Feb. 2013.